The Astrophysical Journal, 665:1371–1380, 2007 August 20

HALL INSTABILITY OF THIN WEAKLY IONIZED STRATIFIED KEPLERIAN DISKS

Yuri M. Shtemler, Michael Mond, and Edward Liverts
Department of Mechanical Engineering, Ben-Gurion University of the Negev, P.O. Box 653,
Beer-Sheva 84105, Israel; shtemler@bgu.ac.il
Received 2006 November 8; accepted 2007 May 9

ABSTRACT

The stratification-driven Hall instability in a weakly ionized polytropic plasma is investigated in the local approximation within an equilibrium Keplerian disk of a small aspect ratio ϵ. The leading order of the asymptotic expansions in ϵ is applied to both equilibrium and perturbation problems. The equilibrium disk with an embedded purely toroidal magnetic field is found to be stable to radial perturbations and unstable to vertical short-wave perturbations. The marginal stability surface was found in the space of the local Hall and inverse plasma-β parameters, as well as the free parameter of the model related to the total current. To estimate the minimal values of the equilibrium magnetic field that leads to the instability, it was constructed as a sum of a current free magnetic field and the simplest approximation for magnetic field created by the distributed electric current.

Subject headings: instabilities — magnetic fields — planetary systems: protoplanetary disks

1. INTRODUCTION

The dynamics of thin rotating gaseous disks under the influence of a magnetic field is of great importance to numerous astrophysical phenomena. Of particular importance is the study of the various instabilities that may arise within the disks whose inverse growth rates are comparable to the rotation period. The rediscovery of the magnetorotational instability (MRI) within an astrophysical context (Balbus & Hawley 1991) gave the sign to a series of extensive investigations of hydromagnetic instabilities of rotating disks.

While most of the research has focused on the magnetohydrodynamic (MHD) description of MRIs, the importance of the Hall electric field to such astrophysical objects as protoplanetary disks has been pointed out by Wardle (1999). Since then, such works as Balbus & Terquem (2001), Salmeron & Wardle (2003, 2005), Desch (2004), Urpin & Rudiger (2005), and Rudiger & Kitchatinov (2005) have shed light on the role of the Hall effect in the modification of the MRIs. However, in addition to modifying the MRIs, the Hall electromotive force gives rise to a new family of instabilities in a density-stratified environment. That new family of instabilities is characterized by the Hall parameter $\hat{\xi}$ of the order of unity ($\hat{\xi}$ is the ratio of the Hall drift velocity $V_{\rm HD}$ to the characteristic velocity, where $V_{\rm HD} = l_i^2\Omega_i/H_*$, l_i and Ω_i are the inertial length and Larmor frequency, respectively, of the ions, and H_* is the density inhomogeneity length; see Huba 1991; Liverts & Mond 2004; Shtemler & Mond 2006). As shown by Liverts & Mond (2004) and by Kolberg et al. (2005), the Hall electric field combined with density stratification gives rise to two modes of wave propagation. The first one is the stable fast magnetic penetration mode, while the second is a slow quasi-electrostatic mode that may become unstable for a short-enough density inhomogeneity length H_*. The latter is termed the Hall instability, and the aim of the present work is to introduce it within an astrophysical context.

Although the magnetic field configuration in real disks is largely unknown, observations and numerical simulations indicate that the toroidal magnetic component may be of the same order of magnitude as, or some times dominate, the poloidal field due to the differential rotation of the disk, even if the magnetic field is created continuously from an initial purely poloidal field (see, e.g., Terquem & Papaloizou 1996; Papaloizou & Terquem 1997; Hawley & Krolik 2002; Proga 2003).

The present study of the Hall instability is carried out for thin equilibrium Keplerian disks with embedded purely toroidal magnetic fields. While the accepted approach to the steady state of the rotating disks in most astrophysics-related hydromagnetic stability researches is that of a "cylindrical disk," a more realistic model of thin disks is adopted in the current work. Thus, an asymptotic approach developed for equilibrium nonmagnetized rotating disks (Regev 1983; Kluźniak & Kita 2000; Umurhan et al. 2006) is employed here in order to construct a family of steady state solutions for the rotating disks in a toroidal magnetic field within the Hall MHD model and to further the study of their stability. It is shown that in such radially stratified systems the Hall instability indeed occurs with the inverse growth rate of the order of the rotation period.

The paper is organized as follows. The dimensionless governing equations are presented in § 2. In § 3 the Hall MHD equilibrium configuration of a rotating disk subjected to a gravitational potential of a central body and a toroidal magnetic field is described in the thin-disk limit. Linear analysis of the Hall stability of toroidal magnetic fields in thin equilibrium Keplerian disks and the results of calculations for both arbitrary and specific magnetic configurations are presented in § 4. Summary and conclusions are given in § 5.

2. THE PHYSICAL MODEL. BASIC EQUATIONS

2.1. *Dimensional Basic Equations*

The stability of radially and axially stratified thin rotating disks threaded by a toroidal magnetic field under short-wave perturbations is considered. Viscosity and radiation effects are ignored. The Hall electric field is taken into account in the generalized Ohm's law which is derived from the momentum equation for the electron fluid neglecting the electron inertia and pressure. Under the assumptions mentioned above, the dynamical equations that describe the partially ionized plasmas are

$$\frac{\partial n}{\partial t} + \nabla \cdot (n\boldsymbol{V}) = 0, \tag{1a}$$

$$m_i n \frac{D\boldsymbol{V}}{Dt} = -\nabla P + \frac{1}{c}\boldsymbol{j}\times\boldsymbol{B} - m_i n \nabla\Phi, \tag{1b}$$

$$\frac{D}{Dt}(Pn^{-\gamma}) = 0, \tag{1c}$$

$$\frac{\partial \boldsymbol{B}}{\partial t} + c\nabla \times \boldsymbol{E} = 0, \quad \nabla \cdot \boldsymbol{B} = 0, \tag{1d}$$

$$\boldsymbol{E} = -\frac{1}{c}\boldsymbol{V} \times \boldsymbol{B} + \frac{1}{ec}\frac{\boldsymbol{j} \times \boldsymbol{B}}{n_e}, \quad \boldsymbol{j} = \frac{c}{4\pi}\nabla \times \boldsymbol{B}. \tag{1e}$$

Cylindrical coordinates (r, θ, z) are adopted throughout the paper with the associated unit basic vectors $(\boldsymbol{i}_r, \boldsymbol{i}_\theta, \boldsymbol{i}_z)$; t is time; Φ is the gravitational potential of the central object; $\Phi(R) = -GM/R$; $R^2 = r^2 + z^2$; G is the gravitational constant; M is the total mass of the central object; c is the speed of light; e is the electron charge; $\boldsymbol{E}$ and $\boldsymbol{B}$ are the Hall electric and magnetic fields; $\boldsymbol{j}$ is the electrical current density; $\boldsymbol{V}$ is the plasma velocity; $D/Dt = \partial/\partial t + (\boldsymbol{V} \cdot \nabla)$ is the material derivative; n is the number density; $P = P_e + P_i + P_n$ is the total plasma pressure; P_k and m_k are the species pressures and masses ($k = e, i, n$); and subscripts e, i, and n denote the electrons, ions, and neutrals. In compliance with the observation data for protoplanetary disks, the density decreases outward from the center of the disk according to the law $n \sim 1/r^\sigma$ with the density exponent $\sigma \approx 2.75$ (Guilloteau & Dutrey 1998). In a polytropic model of plasmas $\sigma = 3/(\gamma - 1)$, this yields the specific heat ratio $\gamma \approx 2.1$ that is somewhat higher than the standard value $\gamma = 5/3$ used here. It should be noted, however, that in reality the gas temperature is set by a variety of heating and cooling processes, so that the commonly used isothermal law and the polytropic equation of state are rather model simplifications of the problem. Thus, a polytropic equation of state used here only indicates that the polytropic equation of state is compatible with admissible data based on indirect measurements with rather poor spatial resolution. Since the plasma is assumed to be quasi-neutral and weakly ionized,

$$n_e \approx n_i \approx \alpha n_n, \quad n \approx n_n. \tag{2}$$

This indicates the increasing role of the Hall effect in the generalized Ohm law with vanishing ionization degree, $\alpha = n_e/(n_e + n_n) \ll 1$.

2.2. *Scaling Procedure*

The physical variables are now transformed into a dimensionless form,

$$f_{\rm nd} = f/f_*, \tag{3}$$

where f and $f_{\rm nd}$ stand for any physical dimensional and nondimensional variables, while the characteristic scales f_* are defined as

$$V_* = \Omega_* r_*, \quad t_* = \frac{1}{\Omega_*}, \quad \Phi_* = V_*^2,$$
$$m_* = m_i, \quad n_* = n_n, \quad n_{*i} = \alpha n_*, \tag{4a}$$

$$P_* = K(m_* n_*)^\gamma, \quad j_* = \frac{c}{4\pi}\frac{B_*}{r_*}, \quad E_* = \frac{V_* B_*}{c}, \tag{4b}$$

where $\Omega_* = (GM/r^3)^{1/2}$ is the value of the Keplerian angular velocity of fluid at the characteristic radius r_* and K is the dimensional constant in the steady state dimensional polytropic law. The characteristic values of the magnetic field B_* and radius r_* are the dimensional parameters of the problem. Note that the relations from equations (4a) and (4b) determine the characteristic magnitudes of the equilibrium density, magnetic field, and velocity for any given value of the characteristic radius within the disk (the equilibrium velocity is determined by Keplerian law, while density and magnetic field are given by eq. [36]). This yields the dimensionless system (omitting the subscript "nd" in nondimensional variables),

$$\frac{\partial n}{\partial t} + \nabla \cdot (n\boldsymbol{V}) = 0, \tag{5a}$$

$$n\frac{D\boldsymbol{V}}{Dt} = -\frac{1}{M_S^2}\nabla P + \frac{1}{\beta M_S^2}\boldsymbol{j} \times \boldsymbol{B} - n\nabla\Phi,$$
$$\Phi(r, z) = -\frac{1}{(r^2 + z^2)^{1/2}}, \tag{5b}$$

$$\frac{D}{Dt}(Pn^{-\gamma}) = 0, \tag{5c}$$

$$\frac{\partial \boldsymbol{B}}{\partial t} + \nabla \times \boldsymbol{E} = 0, \quad \nabla \cdot \boldsymbol{B} = 0, \tag{5d}$$

$$\boldsymbol{E} = -\boldsymbol{V} \times \boldsymbol{B} + \xi\frac{\boldsymbol{j} \times \boldsymbol{B}}{n}, \quad \boldsymbol{j} = \nabla \times \boldsymbol{B}, \tag{5e}$$

where M_S is the Mach number, β is the plasma-β, and ξ is the Hall coefficient,

$$M_S = \frac{V_*}{c_{S*}}, \quad \beta = 4\pi\frac{P_*}{B_*^2}, \quad \xi = \frac{\Omega_i}{\Omega_*}\left(\frac{l_i}{r_*}\right)^2 \equiv \frac{B_* c}{4\pi e\alpha n_* \Omega_* r_*^2}, \tag{6}$$

$c_{S*} = (\gamma P_*/n_*)^{1/2}$, $l_i = c/\omega_{pi}$ and $\Omega_i = eB_*/(m_* c)$ are the inertial length and the Larmor frequency of ions, respectively, and $\omega_{pi} = (4\pi e^2 n_{*i}/m_*)^{1/2}$ is the plasma frequency of the ions. Finally, it should be noted that generally, the masses of the ions and the neutrals are not equal. In those cases, another factor should be introduced that characterizes the appropriate ratio. Here, however, we assume for simplicity that that factor is unity.

A common property of thin Keplerian disks is their highly compressible motion with large Mach numbers M_S,

$$\frac{1}{M_S} = \epsilon \ll 1, \quad \epsilon = \frac{H_*}{r_*}, \tag{7}$$

where ϵ is the aspect ratio of the disk and H_* is a characteristic dimensional thickness of the disk. It is convenient therefore to use a stretched vertical coordinate

$$\zeta = \frac{z}{\epsilon}, \quad h = \frac{H}{\epsilon}. \tag{8}$$

3. EQUILIBRIUM SOLUTION IN THIN-DISK LIMIT FOR TOROIDAL MAGNETIC CONFIGURATION

The steady state equilibrium of rotating magnetized disks can now be obtained to leading order in ϵ by writing all physical quantities as asymptotic expansions in small ϵ (similar to Regev [1983], Kluźniak & Kita [2000], and Umurhan et al. [2006] in their analysis of accretion disks, see also references therein). The expressions obtained for the gravitational potential and for the azimuthal velocity express the fact that under the scalings from equations (7) and (8) the magnetic field is weak, so the magnetic pressure cannot provide significant radial support against gravity. This yields for the gravitational potential in the Keplerian portion of the disk

$$\Phi(r, \zeta) = -\frac{1}{r} + \epsilon^2\frac{\zeta^2}{2r^3} + O(\epsilon^4). \tag{9}$$

Then to zeroth order in ϵ, the toroidal velocity V_θ is described by the Keplerian law

$$V_\theta = \Omega(r) r, \quad \Omega(r) = r^{-3/2}, \tag{10}$$

the rest of the velocity components are of higher order in ϵ and can be neglected in constructing the equilibrium solution which provides the basis for the stability study. Let us assume now that the magnetic field is purely toroidal and depends on both r and z,

$$\boldsymbol{B} = B_\theta(r,z)\boldsymbol{i}_\theta, \quad \boldsymbol{j} = \hat{\nabla}\times\boldsymbol{B}, \tag{11a}$$

$$\hat{\nabla} = \boldsymbol{i}_r\frac{\partial}{\partial r} + \frac{1}{\epsilon}\boldsymbol{i}_z\frac{\partial}{\partial \zeta},$$

$$\boldsymbol{j} = (j_r, 0, j_z) = \left[-\frac{1}{\epsilon}\frac{\partial B_\theta}{\partial \zeta}, 0, \frac{1}{r}\frac{\partial (rB_\theta)}{\partial r}\right]. \tag{11b}$$

Since the vector product of the two toroidal vectors $\boldsymbol{V}$ and $\boldsymbol{B}$ is zero, it follows from the system of equations (1a)–(1e) that the Hall electric field has the potential ϕ,

$$\frac{\boldsymbol{j}\times\boldsymbol{B}}{n} = \hat{\nabla}\phi, \tag{12a}$$

or equivalently,

$$n\frac{\partial\phi}{\partial r} = -\frac{B_\theta}{r}\frac{\partial (rB_\theta)}{\partial r}, \quad n\frac{\partial\phi}{\partial\zeta} = -B_\theta\frac{\partial B_\theta}{\partial\zeta}. \tag{12b}$$

Substituting equations (12a) and (12b) into the vertical component of the momentum equation (5b) yields in the leading order in ϵ

$$c_S = \sqrt{\gamma\frac{P}{n}}, \quad P = n^\gamma,$$

$$n = \nu\left[\frac{\phi(r,\zeta)}{\beta} + \frac{h^2-\zeta^2}{r^3}\right]^{1/(\gamma-1)}, \quad \nu = \left(\frac{\gamma-1}{2\gamma}\right)^{1/(\gamma-1)}. \tag{13}$$

Here h is the disk thickness where n and ϕ equal zero,

$$n = 0, \quad \phi = 0 \text{ at } \zeta = h, \tag{14}$$

and $h(r)$ is scaled so that $h(1) = 1$; $h(r)$ should be specified to close the problem (see § 4).

Finally, a general expression for the toroidal magnetic field as well as for the Hall potential can be derived by solving the induction equation that assumes the form

$$\frac{\partial(r^2 n)}{\partial\zeta}\frac{\partial(r^2 B_\theta^2)}{\partial r} - \frac{\partial(r^2 n)}{\partial r}\frac{\partial(r^2 B_\theta^2)}{\partial\zeta} = 0. \tag{15}$$

This equation is satisfied for rB_θ that is an arbitrary function of N (Kadomtsev 1976), where N has the meaning of the inertial moment density (see additionally § 4.3),

$$B_\theta = r^{-1} I(N), \quad N = r^2 n. \tag{16}$$

This yields for the Hall potential

$$\phi(N) = -\int_0^N \frac{I(N)\dot{I}(N)}{N}\, dN, \tag{17}$$

where the arbitrary constant in the potential is chosen from the condition that the potential is zero at the disk edge where $n = 0$, i.e., $\phi(0) = 0$; the dot denotes a derivative with respect to the argument. If the arbitrary function $I(N)$ is given, then equations (13) and (17) constitute implicit algebraic equations for the number density n and the potential ϕ.

4. HALL INSTABILITY OF THIN KEPLERIAN DISKS

The stability properties of the axially symmetric steady state equilibrium solutions for thin Keplerian disks are investigated now under small axially symmetric perturbations, and we find the dispersion relation in the short-wave limit.

4.1. *Thin-Disk Approximation for Perturbed Problem*

We start by linearizing the Hall MHD equations (5a) and (5b) about the equilibrium solution within the Keplerian portion of the thin disk. For that purpose, the perturbed variables are given by

$$\overline{F}(r,z,t) = F(r,\zeta) + F'(r,\zeta,t), \tag{18}$$

where $\overline{F}$ stands for any of the physical variables, F denotes the equilibrium value, while F' denotes the perturbations of the form

$$\boldsymbol{B}'(r,z) = B'_\theta\boldsymbol{i}_\theta, \quad \boldsymbol{j}' \approx \left(\frac{1}{\epsilon}\frac{\partial B'_\theta}{\partial\zeta}, 0, \frac{\partial B'_\theta}{\partial r}\right), \quad \boldsymbol{V}' = (0,0,V'_z). \tag{19}$$

Here the velocity perturbations are assumed to be in the z-direction only. These kinds of perturbations provide a particular solution for the linearized equations (5a) and (5b).

Inserting the relations from equations (18)–(19) into equations (5a) and (5b), linearizing them about the equilibrium solution, and applying the principle of the least possible degeneracy of the problem (Van Dyke 1964) to the result, we obtain that B'_θ is of the order ϵ^0, while the axial perturbed velocity V'_z is of the order ϵ^1 and should be rescaled. Furthermore, we rescale the Hall parameter, keeping in mind that it should be of the order of ϵ^1, since its higher and lower limits in ϵ lead to more degenerate problems. Thus, rescaling the axial perturbed velocity and Hall parameter, we derive

$$\hat{V}'_z = \frac{V'_z}{\epsilon}, \quad \hat{\xi} = \frac{\xi}{\epsilon} \equiv \frac{\Omega_i l_i^2}{\Omega_* r_* H_*}, \tag{20}$$

where the rescaled Hall parameter $\hat{\xi}$ is equal to the ratio of the Hall drift velocity $V_{\rm HD}$ to the characteristic velocity $V_* = \Omega_* r_*$, and the characteristic disk thickness $H_* = \epsilon r_*$ (see eq. [7]) is the density inhomogeneity length. It is noted that the limit $\hat{\xi} \ll 1$ yields the MHD model. Finally, this leads to the following linearized system in the leading order in ϵ:

$$\frac{\partial n'}{\partial t} + n\frac{\partial\hat{V}'_z}{\partial\zeta} + \frac{\partial n}{\partial\zeta}\hat{V}'_z = 0, \tag{21a}$$

$$n\frac{\partial\hat{V}'_z}{\partial t} = -\frac{\partial P'}{\partial\zeta} - \frac{1}{\beta}\frac{\partial B_\theta}{\partial\zeta}B'_\theta - \frac{1}{\beta}B_\theta\frac{\partial B'_\theta}{\partial\zeta}, \tag{21b}$$

$$\frac{\partial P'}{\partial t} - c_S^2\frac{\partial n'}{\partial t} = 0, \tag{21c}$$

$$\frac{\partial B'_\theta}{\partial t} + \frac{\partial(B_\theta\hat{V}'_z)}{\partial\zeta} + \hat{\xi}\frac{B_\theta}{n^2}\left[\frac{1}{r}\frac{\partial(rB_\theta)}{\partial r}\frac{\partial n'}{\partial\zeta} - \frac{1}{r^2}\times\frac{\partial(r^2 n)}{\partial r}\frac{\partial B'_\theta}{\partial\zeta} + \frac{\partial n}{\partial\zeta}\frac{\partial B'_\theta}{\partial r} - \frac{\partial B_\theta}{\partial\zeta}\frac{\partial n'}{\partial r}\right] + \hat{\xi}\Psi = 0, \tag{21d}$$

where the perturbed toroidal magnetic field identically satisfies the relation $\nabla \cdot \boldsymbol{B}' = 0$ and Ψ denotes the terms in the magnetic induction equation that do not include derivatives of perturbations. The latter will be neglected below in the short-wave limit, and it is not presented here for brevity.

4.2. *Dispersion Relation in the Short-Wave Limit*

The perturbed quantities are assumed to satisfy the following conditions,

$$\left|\frac{1}{F'}\frac{\partial F'}{\partial t}\right| \sim \left|\frac{1}{F'}\frac{\partial F'}{\partial \zeta}\right| \sim \left|\frac{1}{F'}\frac{\partial F'}{\partial r}\right| \gtrsim \left|\frac{1}{F}\frac{\partial F}{\partial \zeta}\right| \sim \left|\frac{1}{F}\frac{\partial F}{\partial r}\right| \sim \frac{1}{r} \sim 1. \tag{22}$$

This allows us to assume the local approximation for the perturbations

$$F'(r,\zeta,t) = f' \exp\left(-i\omega t + ik_r r + ik_\zeta \zeta\right), \tag{23}$$

where f' denotes the amplitude of fluctuations about the equilibrium; ω is the (generally complex) frequency of perturbations; and $\hat{\boldsymbol{k}} = (k_r, k_\zeta)$ is the wavevector in the scaled coordinates (r,ζ). It should be distinguished from the wavevector $\boldsymbol{k} = (k_r, k_z)$ in the (r,z) coordinates, with $k_z = k_\zeta/\epsilon$. The conditions from equation (22) can now be written as

$$\omega \sim k_\zeta \sim k_r \gtrsim \left|\frac{1}{F}\frac{\partial F}{\partial \zeta}\right| \sim \left|\frac{1}{F}\frac{\partial F}{\partial r}\right| \sim \frac{1}{r} \sim 1. \tag{24}$$

Using equations (23)–(24), the system of equations (21a)–(21d) can be presented as the following system of homogeneous linear algebraic equations:

$$-\hat{C}n' + n\hat{V}_z' = 0, \tag{25a}$$

$$-\hat{C}n\hat{V}_z' = -P' - \beta^{-1}B_\theta B_\theta', \quad V_r' = 0, \tag{25b}$$

$$P' = c_S^2 n', \tag{25c}$$

$$\hat{C}B_\theta' + B_\theta \hat{V}_z' + \hat{\xi}\frac{B_\theta}{n^2}\left[\frac{1}{r}\frac{\partial (rB_\theta)}{\partial \rho}n' - \frac{1}{r^2}\frac{\partial (r^2 n)}{\partial \rho}B_\theta'\right] = 0, \tag{25d}$$

where the scaled phase velocity $\hat{C} = \omega/k_\zeta$ in the scaled coordinates (r,ζ) is related to the phase velocity C in the cylindrical coordinates (r,z) as $\hat{C} = C/\epsilon$, and

$$l_\zeta \frac{\partial}{\partial \rho} = l_\zeta \frac{\partial}{\partial r} - l_r \frac{\partial}{\partial \zeta}, \quad l_r = \frac{k_r}{\hat{k}}, \quad l_\zeta = \frac{k_\zeta}{\hat{k}}, \quad \hat{k} = \sqrt{k_r^2 + k_\zeta^2}. \tag{26}$$

Note that since the radial wavenumber k_r is contained only in the Hall term in the magnetic induction equation (25d), in the leading order in ϵ the standard MHD problem is free from $\hat{k}_r$.

The system of equations (25a)–(25d) has nontrivial solutions if the following cubic eigenvalue equation for the local value of the rescaled phase velocity c is satisfied,

$$Xc^3 + Xc^2 - c - q = 0. \tag{27}$$

Parameters X and q are expressed through the local values of the plasma-β b, Hall coefficient x, and new parameter g, whose the physical meaning will be elucidated later, as

$$c = \frac{\hat{C}}{xc_S}, \quad X = \frac{x^2}{1+b^{-1}}, \quad q = \frac{1+gb^{-1}}{1+b^{-1}}, \tag{28a}$$

$$b^{-1} = \beta^{-1}\frac{B_\theta^2}{c_S^2 n}, \quad x = \hat{\xi}\frac{B_\theta}{c_S n^2}\frac{1}{r^2}\frac{\partial N}{\partial \rho}, \quad g = \frac{d\ln I(N)}{d\ln N}, \tag{28b}$$

where B_θ and N are determined in equations (16). Straightforward analysis of the dispersion relation from equation (27) (such a dispersion relation for the Hall instability of plasma in slab geometry has been derived and investigated in Brushlinskii & Morozov [1980]) reveals that the system is stable for $0 \le q \le 1$, while the instability may occur for the two regimes

$$(1)\ q > 1, \quad X^- < X < X^+ \text{ or } (2)\ q < 0, \quad X > X^-. \tag{29}$$

Here the first instability regime corresponds to $g > 1$, and the second one corresponds to $g < -b$ (see eq. [28a]); X^- and X^+ are the roots of the quadratic equation

$$4qX^2 + (1 + 18q - 27q^2)X + 4 = 0. \tag{30}$$

Although equation (30) provides for the dependence of the local Hall parameter X versus q, it is more convenient to use X as a function of the local plasma-β b and the free parameter g, which may be related to the natural parameter of the disk total current through the disk (see § 4.3). As a first result, it is noticed that the current free magnetic configuration with $g \equiv 0$ is stable, since $0 < q < 1$. In addition, it is noted that the quantities X and q (or equivalently, X, g, and b), which determine the stability properties of the disk, depend on the local values of the equilibrium number density and magnetic field which are determined in § 3 up to the free function $I(N)$ of the inertial moment density.

Figure 1 depicts the family of the marginal stability curves which correspond to the real roots of equation (30). These curves are presented in the X-b^{-1} plane of the local Hall parameter and inverse plasma-β with a single parameter of the family, g. According to the relations from equation (29), there are two instability regimes (Figs. 1*a* and 1*b*). Thus, in Figure 1*a* the values of X located between the top and bottom branches of the marginal stability curves give rise to the first regime of instability, while the disk is stable if X falls outside that interval. In the limit $b^{-1} \to 0$, we have $q \to 1$, and equation (30) has a double root $X = 1$. This means that in the limit of high plasma-β the instability interval becomes very narrow and the disk is stable. In Figure 1*b*, the values of X located higher than the curve X^- correspond to the second instability regime in equation (29) ($q < 0$ mode), and the disk is stable otherwise.

4.3. *Model Equilibrium Solutions for Toroidal Magnetic Fields*

The marginal stability curves in Figure 1 provide for only a qualitative description of the disk stability, since they are depicted in terms of the local parameters which are determined up to the free function $I(N)$. To estimate qualitatively the stability characteristics of the system, a specific example of a toroidal magnetic field is considered. The free function $I(N)$ is presented as a sum of the current free magnetic field (created by a current localized along the disk axis) and the simplest quadratic approximation for

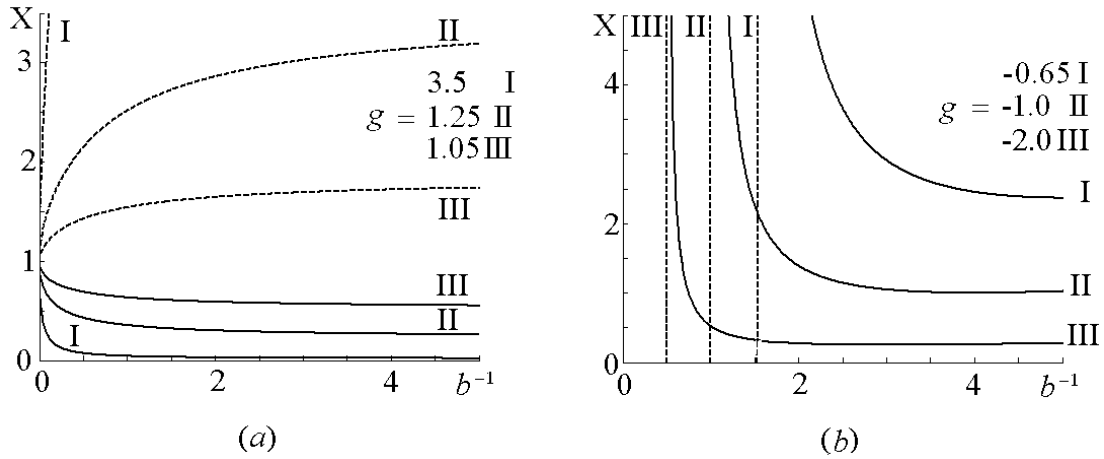

FIG. 1.— Top (*dotted curves*; X^+) and bottom (*solid curves*; X^-) branches of the marginal stability curves in the plane of the local Hall and inverse plasma-β parameters b^{-1}-X for the reference value of radial coordinate $r = 1$ in the midplane $z = 0$ (curves I, II, III for three different values $g \equiv g_0$). Instability region lies either (*a*) between the top and bottom branches ($g > 1$ and $q > 1$) or (*b*) above the bottom branch ($g < 0$ and $q < 0$); dashed straight lines are the vertical asymptotes $q = 0$.

the magnetic field created by an electric current distributed over the Keplerian portion of the disk,

$$I(N) = I_0 + I_2 \frac{N^2}{n_0^2}, \quad N = r^2 n, \tag{31}$$

where I_0 and I_2 are constant coefficients; $n_0 = n(1, 0)$ is the value of the number density at the reference point in the midplane ($r = 1, z = 0$) [analogous notations will be used below for the Hall electric potential $\phi_0 = \phi(1, 0)$, free parameter $g_0 = g(1, 0)$, Hall coefficient $\hat{\xi}_0 = \hat{\xi}(1, 0)$, etc.]. The absence of a linear term in N in equation (31) is a result of the requirement that the Hall electric potential ϕ is finite at the disk edge $z = h$, which in turn allows the number density to be zero.

Substituting equation (31) into equation (17) and using the normalization condition $B_\theta = 1$ at the reference point

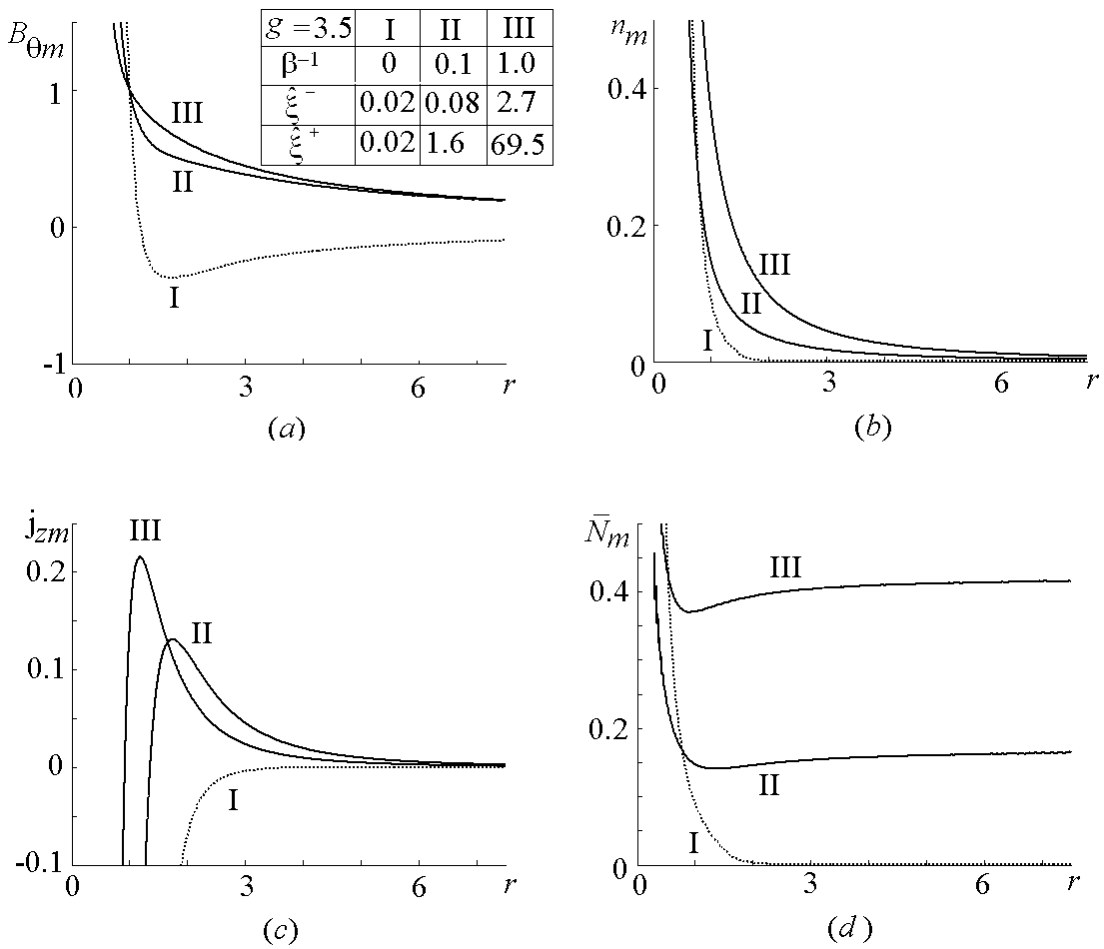

FIG. 2.— Equilibrium midplane profiles of (*a*) the toroidal magnetic field, (*b*) number density, (*c*) distributed electric current, and (*d*) inertial moment density vs. r for $g \equiv g_0 = 3.5$ and three values of the plasma-β (curves I, II, III); $\hat{\xi}^- < \hat{\xi} \equiv \hat{\xi}_0 < \hat{\xi}^+$ belongs to the region of instability.

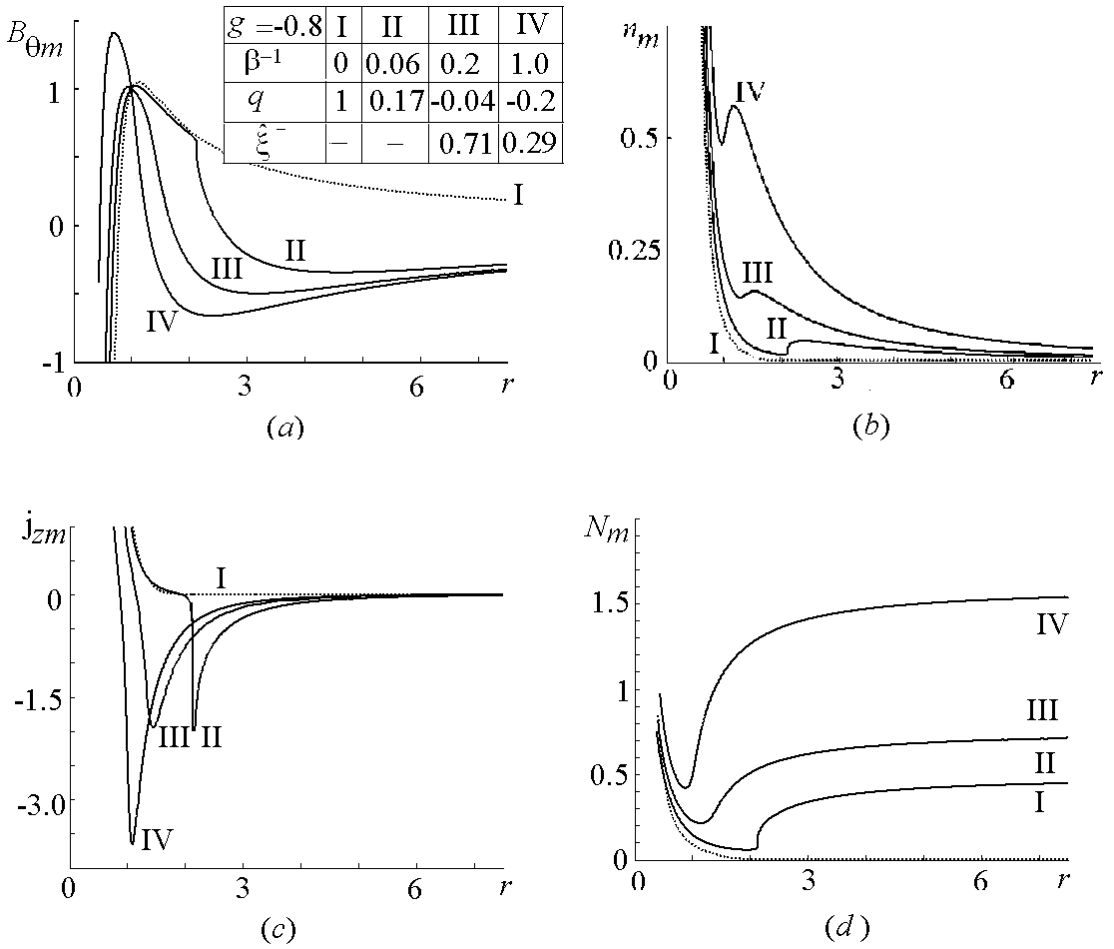

g =-0.8	I	II	III	IV
β^{-1}	0	0.06	0.2	1.0
q	1	0.17	-0.04	-0.2
$\hat{\xi}^-$	–	–	0.71	0.29

FIG. 3.—Same as Fig. 2, but for $g \equiv g_0 = -0.8$; $\hat{\xi}^- < \hat{\xi} \equiv \hat{\xi}_0$ belongs to the region of instability.

($r = 1,\ z = 0$) yield the following expression for the Hall electric potential,

$$\phi(N) = -2I_2 \frac{N}{n_0^2}\left(I_0 + \frac{I_2}{3}\frac{N^2}{n_0^2}\right), \quad I_0 + I_2 = 1. \tag{32}$$

Definitions of g and I in equations (28a)–(28d) and (31) relate the values of I_2, g_0, and the total current through the disk I_t,

$$g_0 = 2I_2, \quad I_t = 2\pi\left[1 - \left(1 - \frac{N_\infty^2}{n_0^2}\right)\frac{g_0}{2}\right], \tag{33}$$

where $N_\infty = (r^2 n_m)_{r\to\infty}$ is constant (see Figs. 2 and 3). This leaves g_0 or, equivalently, the natural parameter of the disk total current I_t as the single free parameter of the model. Equations (13) and (32)–(33) provide for the magnetic configuration in the equilibrium Keplerian disk. To overcome the presence of the arbitrary semithickness $h(r)$ in the relations from equation (13), the small slope of the disk edge is assumed (which is supported by the observation data for some protoplanetary disks; Calvet et al. 2002), such that $h(r) \equiv 1$. This yields at the midplane

$$n_m(r) = \nu\left(\beta^{-1}\phi_m + \frac{1}{r^3}\right)^{1/(\gamma-1)},$$
$$\phi_m(r) = -\frac{g_0 r^2 n_m}{n_0^2}\left[\left(1 - \frac{g_0}{2}\right) + \frac{g_0}{6}\left(\frac{r^2 n_m}{n_0}\right)^2\right], \tag{34}$$

where ν has been defined in equation (13). Equations (34) form a coupled set of nonlinear equations for n_m and ϕ_m, while n_0 is determined from the following two nonlinear equations for $n_0 \equiv n_m(1)$ and $\phi_0 \equiv \phi_m(1)$,

$$n_0 = \nu(\beta^{-1}\phi_0 + 1)^{1/(\gamma-1)}, \quad \phi_0 = -\frac{g_0}{n_0}\left(1 - \frac{g_0}{3}\right). \tag{35}$$

Numerical solution of equations (34) and (35) reveals two main types of equilibria that correspond to two possible signs of g_0, i.e., signs of the contributions of the distributed current to the total current. The midplane equilibrium magnetic field $B_{\theta m}$, number density n_m, distributed electric current j_{zm}, and inertial moment density N_m are presented in Figures 2 and 3 for positive and negative g_0, respectively. In both cases, the equilibria are characterized by a distributed electric current localized at some radius that is moving outward from the disk center with increasing plasma-β. In addition, while for positive g_0 both the equilibrium number density and magnetic field are decreasing monotonically to zero at a finite plasma-β, equilibria with negative g_0 exhibit a maximum in the number density that corresponds to rings of denser material, as well as a maximum in the magnetic field profile. Furthermore, for $g_0 < 0$ the equilibrium solutions exist only for inverse plasma-β larger than a critical value corresponding to the vertical slope ($\beta^{-1} > 0.06$ in Fig. 3); otherwise, the equilibrium solution cannot be described by a single-valued function. It should be noted that for some particular parameters, the equilibrium toroidal magnetic field changes sign at a particular radius. This is

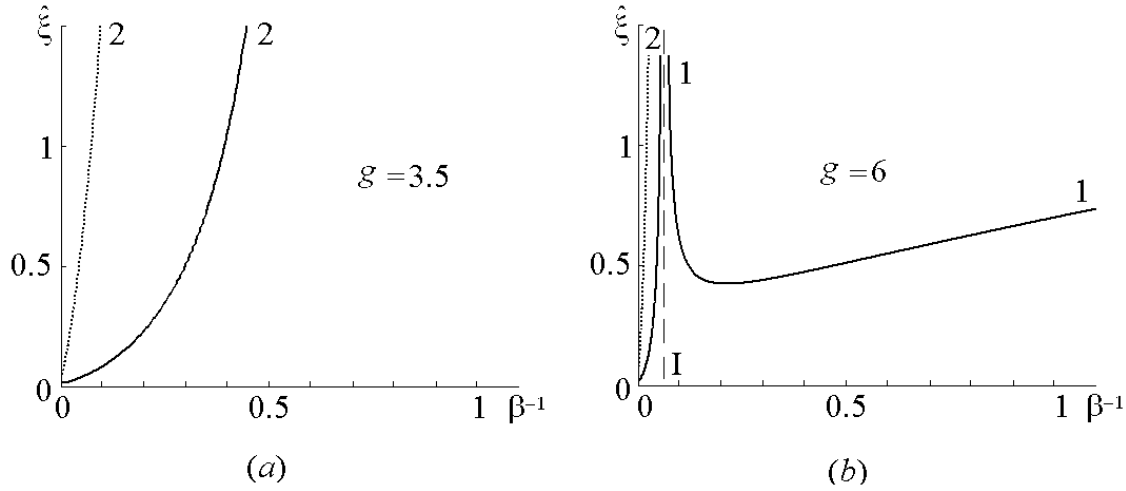

FIG. 4.—Marginal stability curves in the plane of the Hall criterion and inverse plasma-β, β^{-1}-$\hat{\xi}$, for (*a*) $g = 3.5$ and (*b*) 6 ($g \equiv g_0 > 1$, $\hat{\xi} \equiv \hat{\xi}_0$, and reference radius $r = 1$ in the midplane $z = 0$). Dotted and solid curves depict, respectively, the top and bottom branches $\hat{\xi} = \hat{\xi}^{\pm}$ of the marginal stability curves. Dashed lines depict the asymptote I ($\partial_r N_m = 0$) that separates the submodes 1 and 2. The top branch in (*b*) and both branches in (*a*) for the submode 1 are not presented, since they correspond to the Hall parameter $\hat{\xi} > 1.5$.

due to the fact that in those cases the central and the distributed currents are of opposite signs. Finally, Figures 2*d* and 3*d* demonstrate that the inertial moment density N_m tends to a nonzero constant at infinity through a local minimum (critical point) where $\partial_r N_m = 0$.

4.4. *Hall Instability of the Model Equilibrium*

Using the values of the free function $I(N)$ in the magnetic field determined in § 4.3, the family of the marginal stability curves presented in Figure 1 can be recalculated in terms of the Hall coefficient $\hat{\xi}$, the inverse plasma-β β^{-1}, and the free parameter of the model g_0 (i.e., the parameters which are expressed through the input characteristics values of the equilibrium disk; see Figs. 4 and 5).

The values of $\hat{\xi}$ corresponding to the instability (see eq. [29]) lie either between the branches $\hat{\xi}^{-}$ and $\hat{\xi}^{+}$ for $q > 1$ (Figs. 4*a* and 4*b* for $g > 0$) or above the branch $\hat{\xi}^{-}$ for $q < 0$ (Figs. 5*a* and 5*b* for $g < 0$). Then according to the data in Figures 2 and 3, the disk is stable for $\beta^{-1} = 0$, but may become unstable for any finite plasma-β $\beta^{-1} > 0$. Since $\hat{\xi}^{\pm}$ are inversely proportional to the derivative of the inertial moment density $\partial_r N_m$ (see the second relation from eq. [28b] resolved with respect to $\hat{\xi}$), the vertical asymptotes I in Figures 4 and 5 arise if $\partial_r N_m = 0$ at the reference point $r = 1$. As seen in Figures 4 and 5, both positive and negative g modes are subdivided into two submodes 1 and 2 separated by a vertical asymptote I, where $\partial_r N_m = 0$, while the vertical asymptote II, where $q = 0$, bounds the region of instability ($q < 0$ according to eq. [29]) of submode 2.

Figure 6 and equation (24) demonstrate for typical values of the disk parameters that the Hall instability is excited with inverse growth rates of the order of the rotation period (see also § 5). Note that although the angular velocity of the Keplerian rotation drops out from the dimensionless stability problem for the toroidal magnetic configuration, the Keplerian rotation velocity determines the value of the Hall parameter (see eqs. [6]).

Let us estimate the minimal value of the dimensional toroidal magnetic field that corresponds to the onset of the Hall instability. According to the definition of $\hat{\xi}$ in equations (6) and (20),

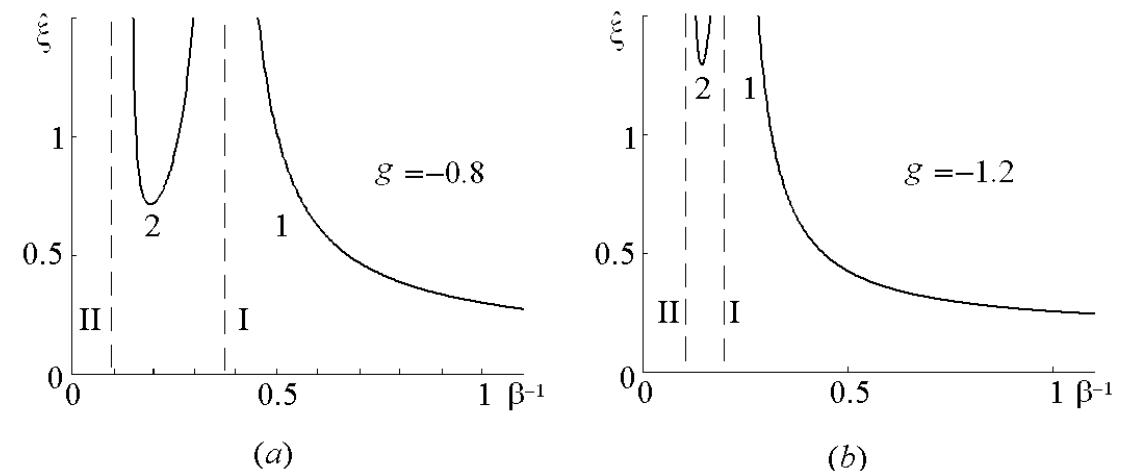

FIG. 5.—Marginal stability curves in the plane of the Hall criterion and inverse plasma-β, β^{-1}-$\hat{\xi}$, for (*a*) $g = -0.8$ and (*b*) -1.2 ($g \equiv g_0 < 0$, $\hat{\xi} \equiv \hat{\xi}_0$, and reference radius $r = 1$ in the midplane $z = 0$). Solid curves depict the marginal stability curves. Dashed lines depict the asymptote I ($\partial_r N_m = 0$), which separates the submodes 1 and 2, and the asymptote II ($q = 0$), which restricts the region of instability for submode 2.

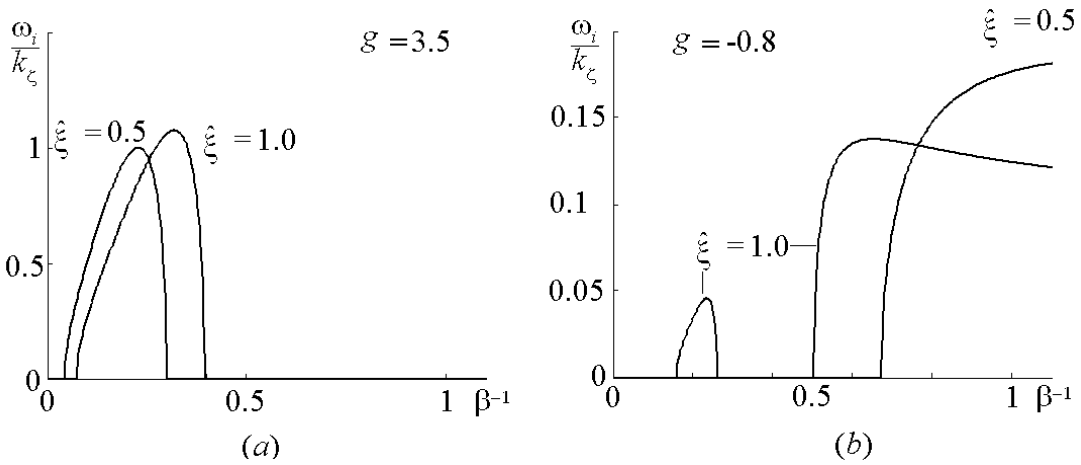

FIG. 6.—Scaled growth rate vs. inverse plasma-β for (*a*) $g = 3.5$ ($q > 1$) and (*b*) $g = -0.8$ ($q < 0$); $g \equiv g_0$, $\hat{\xi} \equiv \hat{\xi}_0$.

the minimal magnetic field that gives rise to the Hall instability is given by (Fig. 7)

$$B_* = \frac{4\pi e n_* (GM)^{1/2}}{c} \epsilon \alpha \hat{\xi} r_*^{1/2}, \tag{36}$$

where $\hat{\xi}$ can be estimated as the characteristic threshold value $\hat{\xi}^-$ that corresponds to the onset of the Hall instability in Figures 4 and 5. Since B_* in equation (36) is proportional to the ionization degree α and the aspect ratio of the disk ϵ, the onset of the Hall instability may occur in weakly ionized and magnetized thin disks.

5. SUMMARY AND CONCLUSIONS

In the present study, a linear analysis of the stratification-driven Hall instability for thin equilibrium Keplerian disks with an embedded purely toroidal magnetic field and hydrostatically equilibrated density has been performed. The stability analysis has been carried out in the short-wave local approximation for the radial and vertical coordinates frozen at the reference point in the midplane, under the assumption of a small slope of the vertical edge of the disk. The leading-order asymptotic expansions in small aspect ratio of the disk are employed in order to construct the Hall MHD equilibrium of the thin Keplerian disks.

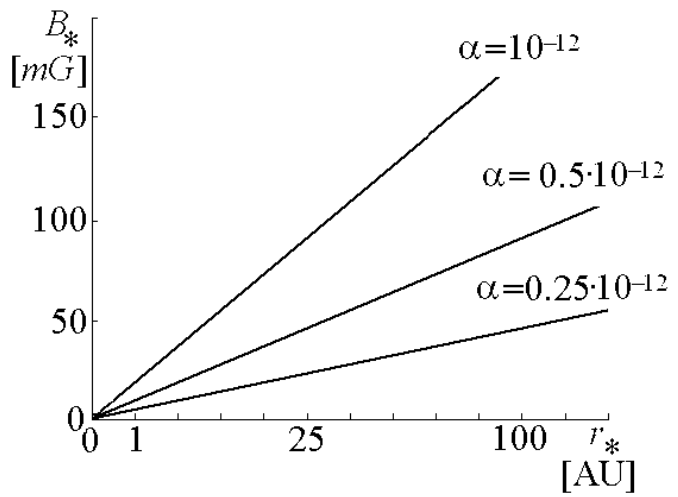

FIG. 7.—Dimensional characteristic toroidal magnetic field in milligauss vs. reference radius in AU for three values of the ionization degree α; $\hat{\xi} \equiv \hat{\xi}_0 = 0.2$; $\epsilon = 0.02$; $n_* \equiv n_n = 10^{12}$ cm^{-3}; and $GM = 1.3 \times 10^{-12}$ cm^3 s^{-2}.

In real protoplanetary disks, the electron density is determined by ionization versus recombination, and the fractional ionization may vary significantly. In such cases, rate equations describing the ionization degree should be employed. However, in the present study the ionization fraction is assumed to be constant with radius within the equilibrium solution as well as for the perturbations. This simplification is made to avoid the widely uncertain physics of ionization and recombination. Nevertheless, such approximation allows one to roughly estimate the real characteristics of the stability. In order to estimate the effect of the spatial variations of the ionization degree, it is noted first that typical ionization rates are much larger than typical rotation frequencies. Hence, since the inverse growth rates of interest are of the order of the rotation period, it is plausible to assume that the system is in ionization equilibrium at each time during the perturbations. Thus, in the presence of trace metal atoms, the equilibrium ionization fraction for constant ionization rate, in two opposite limiting cases of metal absence and of metal domination in the plasma disks, is proportional to the product of powers of the temperature and the neutral number density, $\alpha \sim T^{1/4} n^{-1/2}$ (Urpin & Rudiger 2005; Fromang et al. 2002 and references therein). The latter yields in the polytropic case $\alpha \sim n^{(\gamma-3)/4}$. Now, since the number density variations appear originally in the equilibrium as well as in the linearized equations as $\nabla(\alpha n)$ (in the induction eq. [1d]), the equilibrium gradient in the linearized equation should be multiplied by the same factor $(1 + d \ln \alpha / d \ln n)$, which is of order 1. The latter can range between 1/2 for the isothermal case ($\gamma = 1$) through 2/3 for the adiabatic case ($\gamma = 5/3$) and to 3/4 for $\gamma = 2$, as observed in some protoplanetary disks (see discussion after eqs. [1a]–[1e]). As can be seen from equation (28b), such scale modification would only slightly modify the quantitative Hall instability criteria, as the parameter g is invariant under the scale change and only x is slightly affected by such rescaling. Finally, the input of the perturbed ionization fraction into the Hall mode dynamics can be neglected assuming the characteristic times of ionization and recombination processes are much less than the characteristic times of the Hall perturbations.

It is interesting at this point to compare the Hall instability discussed in the present work with the Hall modified MRI (it is noted that the Hall instability is excited at smaller wavelengths than the MRI). The latter has been investigated in Wardle (1999), Balbus & Terquem (2001), and Rudiger & Shalybkov (2004), and it has been found that MHD unstable MRI modes are stabilized or further destabilized according to whether $\boldsymbol{\Omega} \cdot \boldsymbol{B}$ is positive or negative, respectively. This is due to the fact that the MRI originates

from the interaction of the Alfvèn waves and the inertial (Coriolis) modes. This is in contrast to the Hall instability that represents two other branches of the appropriate dispersion relation, namely, the merging of the slow branch of the fast magnetosonic waves and the slow quasi-electrostatic mode that exists only due to density inhomogeneity (Liverts & Mond 2004). Hence, the Hall instability exists regardless of the mutual orientation of the magnetic field and the rotation. Furthermore, the Hall instability is insensitive to the rotation shear, but rather depends on the density stratification (radial in the case of the current work). It should be noted, however, that Hall modified MRI has been investigated for the case of collinear $\boldsymbol{B}$, $\boldsymbol{\Omega}$, and $\boldsymbol{k}$, while in the present study $\boldsymbol{\Omega} \cdot \boldsymbol{B} = 0$ and $\boldsymbol{k} \cdot \boldsymbol{B} = 0$. Such cases were not investigated before and it is demonstrated here that the Hall electromotive force does indeed give rise to an instability but of a different nature than the MRI which is stable under that configuration.

The linear stability analysis presented in § 4 is local and, hence, is applicable for any arbitrary gradients in equilibrium toroidal magnetic field and density. However, as an illustration and example, full radial and vertical equilibrium profiles have been constructed for the magnetic field and density. It should be remembered, however, that the gradients of magnetic field and density are not totally arbitrary, but are connected by some constraints provided by the equilibrium equations. Indeed, the marginal stability curves depicted in terms of the local parameters in Figure 1 provide for only a qualitative description of the disk stability, since they are determined up to the free function of the total current versus inertial moment density, $I(N)$, and the specific sample of a toroidal magnetic field allows one to estimate quantitatively the stability characteristics of the disk (see Figs. 4 and 5). The Hall electric potential, which determines the equilibrium toroidal magnetic field up to a free function of N, has been modeled as a sum of the current free magnetic field (created by a current localized along the disk axis) and the simplest quadratic approximation for the magnetic field created by the electric current distributed over the Keplerian portion of the disk. The corresponding equilibrium profiles contain a single free parameter, g, of the model that can be expressed through the total current—the natural parameter of the disk. The equilibrium solutions give rise to two types of equilibria that are characterized by opposite signs of g. Thus, negative and positive signs of the latter correspond to distributed currents that are opposite or along the total current, respectively.

The important physical distinctions between the positive and negative g modes of perturbations are demonstrated by their asymptotic behavior with high values of the plasma-β or Hall parameter. Thus, at high values of the Hall parameter the only negative g mode (more exactly negative q mode; see eqs. [28a]–[28b]) is developed, and vice versa at high plasma-β values, the only positive g mode may be excited. Indeed, in accordance with data in Figures 2 and 3 the positive g mode is unstable at arbitrary high plasma-β, while the negative g mode may be unstable starting from a critical value. Whereas in the limit of high values of the Hall parameter ($\hat{\xi}, X \gg 1$), the dispersion relation from equation (27) for the scaled complex phase velocity is reduced in the leading order to $c^2 = q/X$, which is equivalent to $\hat{C}/c_S = i[-(1 + gb^{-1})]^{1/2}$, where g and b are expressed through the equilibrium disk parameters by the relations from equation (28b). This dispersion relation has unstable solutions for only negative g modes ($q < 0$). Other important differences between the positive and negative g modes are demonstrated by comparison of Figures 6*a* and 6*b* at finite values of the Hall parameter and plasma-β. The characteristic times of the perturbation growth for the negative g mode are an order of magnitude longer than for the positive g mode. So the characteristic times of perturbations are much less than the rotation period in the $g > 0$ case, while in the $g < 0$ case they may be much less than (at $k_\zeta \ll 10$) or of the order of (at $k_\zeta \sim 10$) the rotation period. Finally, note that at finite values of the Hall parameter, the positive g mode may become unstable as well as the negative g mode. To estimate the relative magnitudes of the density, magnetic field, and velocity for finite values of the plasma-β and Hall parameter, the eigenvalue $\hat{C}$ (expressed through c found from the cubic dispersion relation from eq. [27]) is substituted into the system of equations (25a)–(25d) for the eigenfunctions. Thus, omitting one of the homogeneous linear algebraic equations in it (e.g., eq. [25d]) yields, using the value $P'/(nc_S^2)$ as the characteristic scale and returning to unscaled in ϵ variables,

$$\frac{n'/n}{P'/nc_S^2} = 1, \quad \frac{V_z'/c_S}{P'/nc_S^2} = \epsilon\frac{\hat{C}}{c_S}, \quad \frac{B_\theta'/B_\theta}{P'/nc_S^2} = \frac{1}{b}\left(1 + \frac{\hat{C}^2}{c_S^2}\right).$$

Thus, in thin-disk approximation, density and magnetic field in the above relations are of order unity, since they are free from the small aspect ratio of the disk in the disk midplane, while the vertical perturbed velocity is small, i.e., of order 1 in ϵ.

It is shown that: (1) the disk that is described by the Hall MHD model is unstable under vertical short-wave perturbations. The Hall instability is demonstrated by the marginal stability surface in the space of the local Hall and inverse plasma-β parameters, as well as the free parameter of the model (Fig. 1). (2) The sign of the free parameter of the model, which may be related to the natural parameter of the disk total current through the disk, determines qualitatively different behavior of both the equilibrium and perturbations (Figs. 2–5). In particular, for negative values of the free parameter, the equilibrium disk exhibits a maximum in the number density that corresponds to rings of denser material, as well as a maximum in the magnetic field (Fig. 3). (3) The disk is stable for the infinite value, but may become unstable for any finite value of plasma-β (Figs. 2 and 3); (4) the current free configuration is shown to be stable, and the existence of the distributed electric current is found to be necessary in order to give rise to the Hall instability; (5) the inverse growth rate is much less than or of the order of the rotation period taken as the characteristic timescale. This is clearly illustrated by Figure 6, where the value of ω_i scaled by the dimensionless wavenumber $k_\zeta \gtrsim 1$ has been made dimensionless by using the Keplerian angular velocity Ω. (6) The density inhomogeneity length is of the order of the characteristic disk thickness; (7) the onset of the Hall instability is possible in thin weakly magnetized and ionized disks (Fig. 7).

This work has been supported by the Israel Science Foundation under contract 265/00. The authors would like to thank an anonymous referee for his careful reading of the manuscript and for his valuable comments and suggestions.

REFERENCES

Balbus, S. A., & Hawley, J. F. 1991, ApJ, 376, 214
Balbus, S. A., & Terquem, C. 2001, ApJ, 552, 235
Brushlinskii, K. V., & Morozov, A. I., 1980, in Reviews of Plasma Physics, ed. M. A. Leontovich (New York: Consultants Bureau), 8, 105
Calvet, N., D'Alessio, P., Hartmann, L., Wilner, D., Walsh, A., & Sitko, M. 2002, ApJ, 568, 1008
Desch, S. J. 2004, ApJ, 608, 509
Fromang, S., Terquem, C., & Balbus, S. A. 2002, MNRAS, 329, 18

Guilloteau, S., & Dutrey, A. 1998, A&A, 339, 467
Hawley, J. F., & Krolik, J. H. 2002, ApJ, 566, 164
Huba, J. D. 1991, Phys. Fluids B, 3, 3217
Kadomtsev, B. B. 1976, Collective Phenomena in Plasma (Moscow: Nauka)
Kluźniak, W., & Kita, D. 2000, ApJ, submitted (astro-ph/0006266)
Kolberg, Z., Liverts, E., & Mond, M. 2005, Phys. Plasmas, 12, 062113
Liverts, E., & Mond, M. 2004, Phys. Plasmas, 11, 55
Papaloizou, J. C. B., & Terquem, C. 1997, MNRAS, 287, 771
Proga, D. 2003, ApJ, 585, 406
Regev, O. 1983, A&A, 126, 146
Rudiger, G., & Kitchatinov, L. L. 2005, A&A, 434, 629
Rudiger, G., & Shalybkov, D. 2004, Phys. Rev. E, 69, 016303
Salmeron, R., & Wardle, M. 2003, MNRAS, 345, 992
———. 2005, MNRAS, 361, 45
Shtemler, Y. M., & Mond, M. 2006, J. Plasma Phys., 72, 669
Terquem, C., & Papaloizou, J. C. B. 1996, MNRAS, 279, 767
Umurhan, O. M., Nemirovsky, A., Regev, O., & Shaviv, G. 2006, A&A, 446, 1
Urpin, V., & Rudiger, G. 2005, A&A, 437, 23
Van Dyke, M. 1964, Perturbation Methods in Fluid Mechanics (New York: Academic)
Wardle, M. 1999, MNRAS, 307, 849